Long noncoding RNA STCAT16 suppresses cell growth and its expression predicts prognosis in patients with gastric cancer

JIAN-FENG ZHANG[1*], WEI JIANG[2*], QIAN-FENG ZHANG[1], XIAO-LING KUAI[1],
ZHEN-BIAO MAO[1] and ZHI-WEI WANG[3]

Departments of [1]Gastroenterology, [2]Emergency Centre and [3]General Surgery,
Affiliated Hospital of Nantong University, Nantong, Jiangsu 226001, P.R. China

Abstract. Gastric cancer (GC) is a leading cause of cancer-associated mortality worldwide. Previous studies demonstrated that long noncoding RNAs (lncRNAs) may be dysregulated in GC and may serve important roles in cancer progression. The present study aimed to investigate the role of the novel lncRNA stomach cancer-associated transcript 16 (STCAT16; Assembly Gene ID G038291) in the development and progression of GC. The present data suggested that the expression level of STCAT16 was decreased in GC tissues. The expression level of STCAT16 was identified to be associated with lymph node and tumour node metastasis stages. Furthermore, the expression level of STCAT16 was identified to be significantly associated with poor survival and prognosis. Knockdown of STCAT16 promoted proliferation, colony formation, migration and invasion of BGC-823 cells. In contrast, these features were suppressed in AGS cells following overexpression of STCAT16. *In vivo*, tumour growth was significantly decreased following STCAT16 overexpression. Collectively, the present data suggested that the lncRNA STCAT16 may act as a tumour suppressor and may inhibit GC tumour cell growth and migration. Additionally, the decreased expression level of STCAT16 was identified to be associated with poor prognosis in patients with GC.

Correspondence to: Professor Zhen-Biao Mao, Department of Gastroenterology, Affiliated Hospital of Nantong University, Building 6, 20 Xisi Road, Chongchuan, Nantong, Jiangsu 226001, P.R. China
E-mail: mzb1963@126.com

Professor Zhi-Wei Wang, Department of General Surgery, Affiliated Hospital of Nantong University, Building 6, 20 Xisi Road, Chongchuan, Nantong, Jiangsu 226001, P.R. China
E-mail: 574267231@qq.com

*Contributed equally

Introduction

Gastric cancer (GC) is one of the most common types of cancer worldwide and is one of the leading causes of cancer-associated mortality, particularly in China (1). Recent advances in diagnosis and treatment have improved the long-term survival rate of patients with early-stage GC; however, the prognosis of patients with late-stage GC remains poor, primarily due to cancer invasion and metastasis (2-5). Tumour invasion and metastasis are progressive, multifactorial and multistep processes that involve cell adhesion and migration, local invasion into the adjacent tissue, intravasation, survival in the circulatory system, extravasation and migration into target organs, where tumour cells may further proliferate (6). The invasion of tumour cells into surrounding tissues is an important early event in GC metastasis (7,8). However, the molecular mechanism underlying GC invasion of surrounding tissues remains unclear. Therefore, investigation of this process is required to improve the understanding of tumour metastasis. The present results may facilitate the identification of novel molecular targets that may be used to develop novel therapeutic strategies to inhibit GC metastasis.

Long noncoding RNAs (lncRNAs) are RNA molecules >200 nucleotides in length. These RNAs have limited coding capability; however, they are involved in various biological processes, including epigenetic modifications (9,10), and transcriptional (11) and post-transcriptional regulation (12). Additionally, putative lncRNAs have been identified to encode small peptides (13). Therefore, lncRNAs may serve various roles in multiple diseases. Accumulating evidence has demonstrated that lncRNAs are dysregulated in various types of cancer, serving important roles in signalling pathways controlling tumourigenesis and cancer progression (14). Multiple lncRNAs, including HOX transcript antisense RNA (HOTAIR) (15,16), gastric carcinoma proliferation enhancing transcript 1 (GHET1) (17), hepatocellular carcinoma upregulated long noncoding RNA (HULC) (18), colon cancer associated transcript 1 (CCAT1) (19) and maternally expressed 3 (MEG3) (20,21), were demonstrated to be associated with GC progression, serving as oncogenes or tumour suppressor genes.

A previous study by Iyer *et al* (22) identified various novel lncRNAs; among these novel lncRNAs, stomach cancer-associated transcript 16 (STCAT16) exhibited a

significant downregulation in GC tissues; however, the association between STCAT16 and clinicopathological characteristics of patients with GC remains unknown. In the present study, the expression level of STCAT16 was identified to be downregulated in GC tissues and cell lines. STCAT16 downregulation was significantly associated with poor clinical features and prognosis. Notably, STCAT16 overexpression inhibited proliferative and invasive abilities of GC cells, and multivariate analysis identified that high expression level of STCAT16 was an independent predictor for improved overall survival (OS) rate in patients with GC.

Materials and methods

Human samples. The present study was approved by The Institutional Review Board of The Affiliated Hospital of Nantong University (Nantong, China) and was performed in accordance with the Declaration of Helsinki. Written informed consent was obtained prior to the start of the study. GC tissues and matched normal gastric tissues, located 5 cm from the tumour margin, were collected from 59 patients with GC (age, 32-84 years; female to male ratio, 24:35) from the Department of General Surgery (Affiliated Hospital of Nantong University) between December 2014 and August 2015. Clinical data and follow-up information were obtained from the medical records of the patients. GC stage was assigned according to the tumour, node and metastasis (TNM) classification and staging system recommended by the American Joint Committee on Cancer (23). T and N classification was based on non-invasive examinations and M classification was determined from samples that were surgically removed. OS was defined as the duration between the date of surgery and the date of mortality or the last follow-up. All patients were followed up until December 2017. The patients did not receive radiation therapy or chemotherapy prior to surgery. Patients included in the study did not exhibit long-term use of nonsteroidal anti-inflammatory drugs or corticosteroids prior to the surgery. Cancer classification and pathological types were assessed by two experienced pathologists in a double-blind manner.

Cell culture and transfection. Human GC cell lines (SGC-7901, MKN-45, AGS, MGC-803 and BGC-823) and a human normal gastric mucosa cell line (GES-1) were purchased from the Shanghai Institutes for Biological Sciences of The Chinese Academy of Sciences (Shanghai, China). Cells were cultured in RPMI-1640 medium (HyClone; GE Healthcare Life Sciences, Logan, UT, USA) containing 10% foetal bovine serum (FBS; Zhejiang Tianhang Biotechnology Co., Ltd., Huzhou, China), 100 μg/ml streptomycin and 100 U/ml penicillin at 37°C with 5% CO_2. Cells in the logarithmic (log) phase were selected and transfected in 24-well plates at 85% confluence using Lipofectamine® 2000 (Invitrogen; Thermo Fisher Scientific, Inc., Waltham, MA, USA). The cells were dissociated using a solution containing 0.25% trypsin-EDTA (Sigma-Aldrich; Merck KGaA, Darmstadt, Germany). Subsequent experiments were performed 72 h post-transfection.

Reverse transcription-quantitative polymerase chain reaction (RT-qPCR). The relative expression level of STCAT16 was determined by RT-qPCR. Total RNA was extracted from 100 mg tissues or cells using TRIzol® (Invitrogen; Thermo Fisher Scientific, Inc.). Subsequently, RNA was reverse-transcribed into cDNA with a Moloney murine leukaemia virus reverse transcriptase kit (Thermo Fisher Scientific, Inc.). The temperature protocol was as follows: 42°C for 60 min, 70°C for 5 min. According to the manufacturer's instructions, qPCR was executed using SYBR-Green I (Takara Biotechnology, Co., Ltd., Dalian, China) and an Applied Biosystems 7500 Real-Time PCR System (Thermo Fisher Scientific, Inc.). The qPCR reaction mixture contained 10 μl SYBR-Green/ROX qPCR Master Mix (Takara Biotechnology, Co., Ltd.), 1 μl forward primers (STCAT16, 5'-CATCAAGGCTTGTGGGAT GT-3'; GAPDH, 5'-CTGGGCTACACTGAGCACC-3'), 1 μl reverse primers (STCAT16, 5'-AAGCCGAAAGGTCAACTG C-3'; GAPDH, 5'-AAGTGGTCGTTGAGGGCAATG-3'), 2 μl cDNA and 6 μl sterile double steamed water. GAPDH was used as a reference gene. The thermocycling conditions were the following: 95°C for 10 min, followed by 40 cycles at 95°C for 15 sec and 60°C for 60 sec. Primers of STCAT16 were synthesized by Shanghai Ruian BioTechnologies Co., Ltd. (Shanghai, China). The data were quantified using the $2^{-\Delta\Delta Cq}$ method (24). Each experiment was performed in triplicate.

STCAT16 knockdown and overexpression vectors construction. A total of four plasmids containing sequences for short hairpin RNAs (shRNAs) targeting STCAT16 (STCAT16-shRNA-759, STCAT16-shRNA-1161, STCAT16-shRNA-1356 and STCAT16-shRNA-1693), a plasmid containing the negative control (NC) shRNA and a STCAT16 overexpression plasmid (STCAT16-pcDNA3.1) were constructed by Shanghai GenePharma Co., Ltd (Shanghai, China). Cells were selected in the logarithmic phase and transfected with 4.0 μg/well plasmid DNA in 24-well plates (5x10^5 cells/well) at 85% confluence using Lipofectamine® 2000 (Invitrogen; Thermo Fisher Scientific, Inc.) according to the manufacturer's protocol. Empty pcDNA3.1 plasmid was used as NC for the overexpression experiments (mock-NC). The plasmid extraction kit was purchased from Omega Bio-tek, Inc. (Norcross, GA, USA).

Cell proliferation assay. Cell proliferation was assessed using the Cell Counting Kit-8 (CCK-8; Beyotime Institute of Biotechnology, Haimen, China) according to the manufacturer's protocol. Cells growing in the exponential phase were plated at a density of 5x10^4 cells/ml on 96-well plates and four plasmids (STCAT16-shRNA, sh-NC and STCAT16-pcDNA3.1, mock-NC) were transfected with 4.0 μg/well per plasmid DNA using Lipofectamine® 2000 (Invitrogen; Thermo Fisher Scientific, Inc.). At 0, 24, 48, 72 and 96 h, 10 μl CCK-8 solution was added to each well followed by a 2-h incubation at 37°C. The absorbance was recorded at 450 nm with a microplate reader (Varioskan® Flash; Thermo Fisher Scientific, Inc.). All experiments were performed in triplicate.

Colony formation assay. Colony formation assays were performed as previously described (25). A total of 4.0 μg/well per plasmid DNA of four plasmids (STCAT16-shRNA, sh-NC and STCAT16-pcDNA3.1, mock-NC) were transfected using Lipofectamine® 2000 (Invitrogen; Thermo Fisher Scientific, Inc.) according to the manufacturer's protocol. Cells were seeded on 6-well plates at a concentration of 100 cells/well

and cultured at 37°C for 2-3 weeks. Surviving colonies were counted following staining with Gentian Violet (Amresco, LLC, Solon, OH, USA) for 5 min at room temperature. Colonies with >50 cells were counted under an upright light microscope (magnification, x100; BX51 Microscope; Olympus Corporation, Tokyo, Japan). All experiments were performed in triplicate.

Wound healing assay. Cells were plated on 6-well plates at a density of 5x10^5 cells/well and four plasmids (STCAT16-shRNA, sh-NC and STCAT16-pcDNA3.1, mock-NC) were transfected with 4.0 µg/well per plasmid DNA using Lipofectamine® 2000 (Invitrogen; Thermo Fisher Scientific, Inc.). The cell monolayers were scratched in a straight line using a pipette tip at 24 h after transfection. The debris was removed with three washes in PBS, and phase-contrast images were acquired using an inverted fluorescence microscope (IX71; Olympus Corporation, Tokyo, Japan; magnification, x100). Cells were cultured for an additional 24 h, and imaged at 6, 12 and 24 h in that incubation period. Subsequently, the number of migrating cells was counted.

Cell invasion assay. STCAT16-shRNA, sh-NC and STCAT16-pcDNA3.1, mock-NC plasmids (all 4.0 µg/well plasmid DNA) were transfected into GC cells using Lipofectamine® 2000 (Invitrogen; Thermo Fisher Scientific, Inc.). The cell suspension containing 1x10^5 cells/ml transfected for 48 h was placed in an upper chamber (Transwell®; Corning Inc., Corning, NY, USA) precoated with Matrigel (BD Biosciences, San Jose, CA, USA). A total of 600 µl RPMI-1640 supplemented with 20% FBS was plated in the lower chamber. Invasive cells were able to pass through the Matrigel layer. Subsequently, cells were incubated for 24 h and stained with crystal violet (Beyotime Institute of Biotechnology) at room temperature for 20 min. The field of view (n=15) of each insert was randomly counted using an upright light microscope (BX51; Olympus Corporation, Tokyo, Japan; magnification, x100) and the average value was calculated.

In vivo tumourigenesis assay. A total of 10 male BALB/c nude mice (age, 4 weeks; weight, 18-20 g) were purchased from The Laboratory Animal Research Centre of Nantong University (Nantong, China). Mice were maintained at 24°C in a temperature-controlled environment with 40-60% relative humidity, under a 12-h light/dark cycle using a dimmer, with food and water *ad libitum*. Mice were randomly divided into two groups (n=5 in each group) and injected with STCAT16-pcDNA3.1-transfected AGS cells (STCAT16-pcDNA3.1 group) or with empty pcDNA3.1-transfected AGS cells (mock-NC group). The 2x10^7 cells were subcutaneously injected into the back of the mice. The mice with developing tumours were observed ≥3 times per week. The tumours were allowed to grow for 4 weeks, and the tumour volume (V) was calculated using the following formula: $V=0.5 \times length \times width^2$. All animal experiments were approved by The Animal Care and Use Committee of Nantong University.

Immunohistochemistry. Tumour tissue sections were fixed in 10% buffered formalin for 24 h at room temperature, embedded in paraffin and cut into 4 µm sections. The sections were deparaffinized in xylene, rehydrated in graded ethanol solutions and treated with 0.1% hydrogen peroxide in methanol for 20 min. Antigen retrieval was performed by microwaving the sections immersed in 10 mM citric acid buffer for 10 min, followed incubation for 1 h at room temperature. Sections were incubated with 5% bovine serum albumin (cat. no. LLBB-1000-01, SurModics, Inc., Eden Prairie, USA) to block non-specific protein binding for 10 min at 37°C, followed by 1-h incubation at room temperature and overnight at 4°C with monoclonal antibody against Ki-67 (1:50 dilution; cat. no. ab16667; Abcam, Cambridge, UK). Sections were washed with PBS and incubated with a horseradish peroxidase-conjugated polyclonal goat anti-rabbit immunoglobulin G biotin secondary antibody (1:500 dilution; cat. no. E030110-01; EarthOx, LLC, San Francisco, CA, USA) for 1 h at room temperature, followed by 0.1% hydrogen peroxide and 0.6 mM 3,3'-Diaminobenzidine (DAB) in PBS for 8 min at room temperature. All sections were stained using a Hematoxylin and Eosin Staining kit (cat. no. C0105; Beyotime Institute of Biotechnology) as previously described (26), and examined using a light microscope (BX51; Olympus Corporation; magnification, x400). The nuclear was stained blue and cytoplasm was stained red.

Regarding assessment, Ki-67 staining intensity was evaluated using a four rating-level-scheme, where scores ranging from 0 to 3 indicated negative, weak, medium and strong staining, respectively. For extent of staining, a five rating-level-scheme was employed. Thus, based on the total amount of positive stained areas in the whole carcinoma region, the extent of staining was evaluated with scores ranging from 0 to 4 as follows: 0, 0; 1, 1-25; 2, 26-50; 3, 51-75; and 4, 76-100%. In each specimen, five high-power fields (x400) were randomly selected, together with examination of nuclear staining. The product of intensity scores multiplied by degree scores was used as the final staining score (0-12) for Ki-67 assessment. The staining was evaluated as previously described (27).

Statistical analysis. All experiments were performed in triplicate. All statistical analyses were performed using SPSS software (version 17.0; SPSS, Inc., Chicago, IL, USA). Graphs were generated using GraphPad Prism software (version 5.0; GraphPad Software, Inc., La Jolla, CA, USA). Data are presented as the mean ± standard deviation. Differences between two groups and in more than two groups were evaluated using a paired Student's t-test and one-way analysis of variance, respectively. Student-Newman-Keuls post hoc test was performed following ANOVA. The association between the expression level of STCAT16 and clinical characteristics was analysed using χ^2 test or Fisher's exact probability. Parameters associated with OS and time to recurrence (TTR) were identified using univariate and multivariate Cox proportional hazards regression models. Kaplan-Meier plots (log-rank test) were used to examine OS and TTR. P<0.05 was considered to indicate a statistically significant difference.

Results

Expression level of STCAT16 is downregulated in human gastric cancer and decreased expression level of STCAT16 is
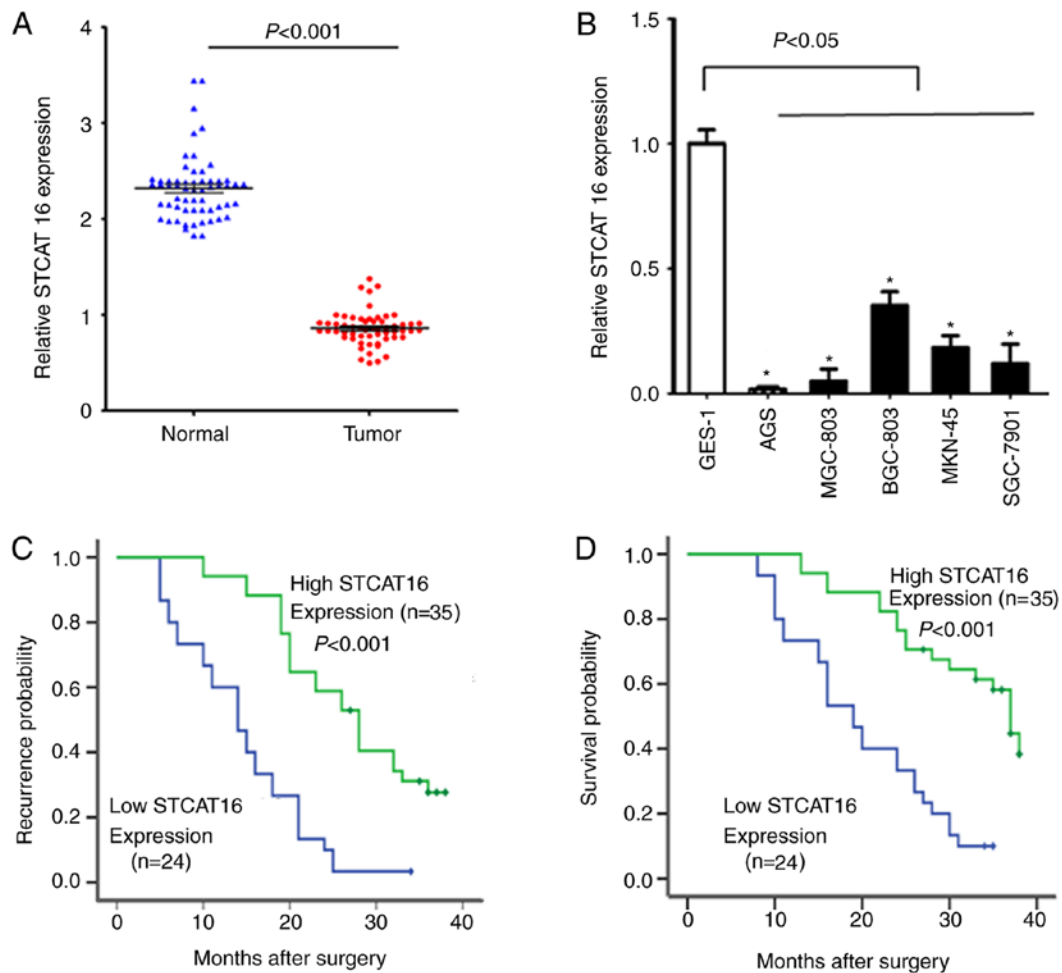
Figure 1. Expression of STCAT16 in GC and its prognostic significance in patients with GC. RT-qPCR was used to detect the expression of STCAT16 in (A) GC tissues and in (B) cell lines. GC cell lines and a human normal gastric mucosa cell line (GES-1) were used for RT-qPCR analysis. (C) Postoperative recurrence and (D) overall survival in patients with increased or decreased expression levels of STCAT16 were assessed by log-rank test. *P<0.05 vs. GES-1 cells. GC, gastric cancer; RT-qPCR, reverse transcription polymerase chain reaction; STCAT16, stomach cancer-associated transcript 16.

associated with poor OS. The expression level of STCAT16 in GC tissues was significantly decreased compared with adjacent normal gastric tissues (Fig. 1A). The expression level of STCAT16 varied among GC cell lines; however, all cell lines exhibited a decreased expression level of STCAT16 compared with GES-1 cells (Fig. 1B). Compared with GES-1 cells, AGS and BGC-823 cells exhibited a relative expression level of STCAT16 of 0.015±0.006 and 0.332±0.056, respectively.

The clinical features of the enrolled patients are listed in Table I. If the expression level of STCAT16 in the tumour tissue was decreased >2-folds compared with the matched adjacent normal tissue, the expression level of STCAT16 was considered as low. The expression level of STCAT16 in GC tissues was identified to be associated with TNM stage and lymph node metastasis. The TTR of patients with low STCAT16 expression was significantly decreased compared with patients exhibiting high STCAT16 expression (Fig. 1C). Additionally, OS was significantly decreased in patients exhibiting low expression level of STCAT16 (Fig. 1D).

To further investigate the prognostic potential of STCAT16, univariate and multivariate survival analyses were performed examining clinicopathological characteristics of patients with GC. The univariate analysis was performed using six prognostic

factors: Age, sex, differentiation degree, lymph node metastasis, TNM stage and STCAT16 expression level. The multivariate analysis identified that the TNM stage and the expression level of STCAT16 were independent predictors of OS (Table II).

STCAT16 interference and overexpression. To identify the most effective shRNA, four STCAT16-shRNAs plasmids were transfected into BGC-823 cell line, which exhibited an increased expression level of STCAT16. Among the four shRNAs, STCAT16-shRNA-759 exhibited the most effective knockdown compared with the negative control (STCAT16-sh-NC) group (Fig. 2A). Therefore, STCAT16-shRNA-759 was used in further experiments.

Furthermore, STCAT16-pcDNA3.1 plasmid was transfected into AGS cells, which exhibited a decreased expression level of STCAT16 compared with other GC cell lines. The expression level of STCAT16 was significantly increased in the STCAT16-pcDNA3.1 group compared with the mock-NC group, which was transfected with an empty vector.

STCAT16 overexpression inhibits gastric cancer cell proliferation and colony formation. To investigate the biological effects of STCAT16 on GC cells, the expression level of STCAT16

Table I. Association between STCAT16 expression and clinical characteristics.

| | | STCAT16 | | |
| | | High (n=35) | Low (n=24) | |
Clinical characteristics	n			P-value
Age (years)				0.598
<60	27	15	12	
≥60	32	20	12	
Sex				0.504
Male	35	22	13	
Female	24	13	11	
Tumour size (cm)				0.679
<5	40	23	17	
≥5	19	12	7	
Tumour, node and metastasis stage				0.027[a]
I/II	20	16	4	
III/IV	39	19	20	
Differentiation degree				0.400
High or medium	26	17	9	
Low	33	18	15	
Lymph node metastasis				0.025[a]
Yes	34	16	18	
No	25	19	6	

[a]P<0.05. If the expression level of STCAT16 in the tumour tissue was decreased >2 fold compared with the matched adjacent normal tissue, the expression level of STCAT16 was considered as low. STCAT16, stomach cancer-associated transcript 16.

Table II. Univariate and multivariate analysis of clinicopathological characteristics and overall survival in 59 patients with gastric cancer.

A, Univariate analysis

Clinical characteristics	Hazard ratio	95% confidence interval	P-value
Age (≥60 and <60)	1.101	0.751-2.451	0.931
Sex	0.461	0.251-1.072	0.442
Differentiation degree (high/middle/low)	0.908	0.742-2.411	0.658
Tumour, node and metastasis stage (I/II/III/IV)	5.455	1.890-11.080	0.055
Lymph node metastasis (no/yes)	0.723	0.818-3.524	0.620
STCAT16 expression level (high/low)	6.560	2.331-17.232	0.018

B, Multivariate analysis

Clinical characteristics	Hazard ratio	95% confidence interval	P-value
Age (≥60 and <60)	1.224	1.331-2.221	0.828
Sex	1.008	0.411-1.722	0.345
Differentiation degree (high/middle/low)	1.244	0.311-3.616	0.120
Tumour, node and metastasis stage (I/II/III/IV)	6.753	1.321-12.381	0.039
Lymph node metastasis (no/yes)	1.232	0.223-2.919	0.237
STCAT16 expression level (high/low)	7.393	1.928-15.156	0.025

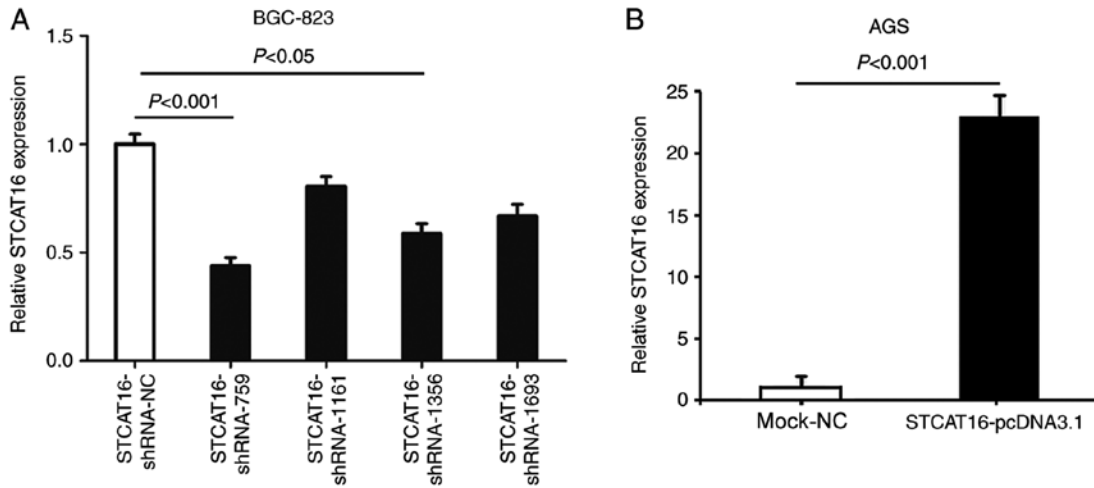STCAT16, stomach cancer-associated transcript 16.

Figure 2. Construction and selection of vectors used to silence or overexpress STCAT16. (A) STCAT16-shRNA-759 exhibited the most effective knockdown of STCAT16 compared with STCAT16-shRNA-NC in BGC-823 cells. (B) Expression level of STCAT16 was significantly upregulated in the STCAT16-pcDNA3.1 group compared with the negative control (mock-NC) group in AGS cells. STCAT16, stomach cancer-associated transcript 16; sh, short hairpin RNA; NC, negative control.
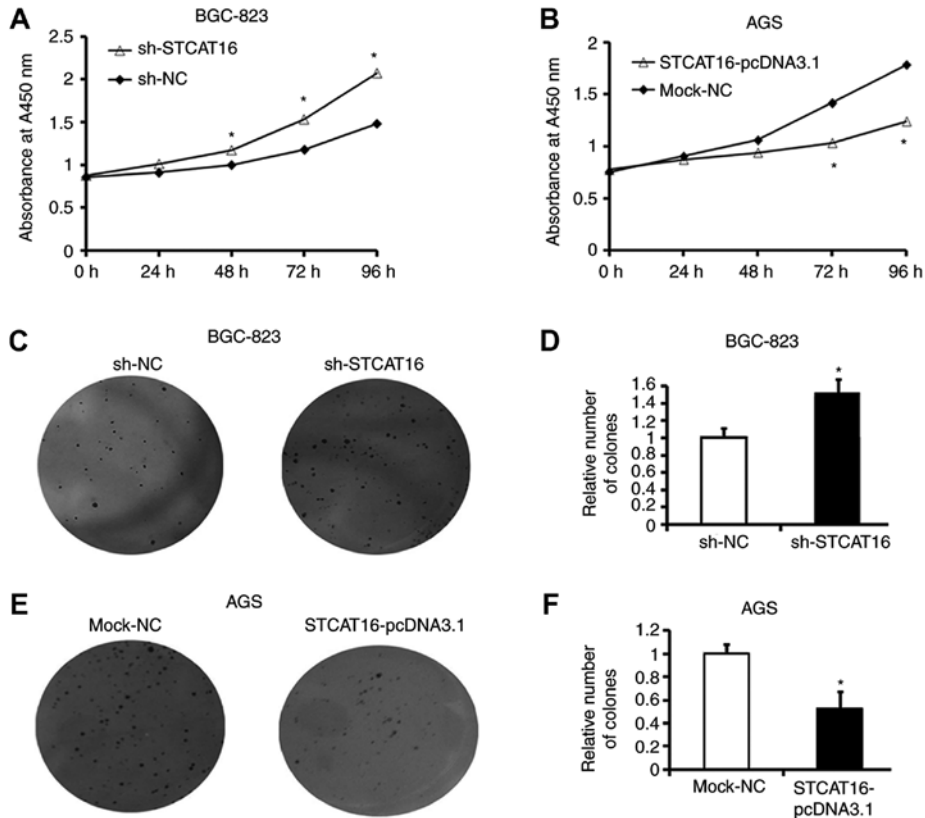

Figure 3. Expression level of STCAT16 affects GC cell proliferation and colony formation *in vitro*. (A) Proliferative ability of BGC-832 cells following STCAT16 knockdown. (B) Proliferative ability of AGS cells following STCAT16 overexpression. (C and D) Colony formation ability of BGC-832 cells following STCAT16 knockdown. (E and F) Colony formation ability of AGS cells following STCAT16 overexpression. Cells in the sh-STCAT16 group were transfected with STCAT16-shRNA-759. Magnification, x100. *P<0.05 vs. corresponding control. STCAT16, stomach cancer-associated transcript 16; sh, short hairpin RNA; NC, negative control.

was silenced by transfecting sh-STCAT16 into BGC-823 cells and overexpressed by transfecting STCAT16-pcDNA3.1 into AGS cells.

Following transfection with sh-STCAT16, the proliferation of BGC-823 cells was significantly increased at 48, 72 and 96 h compared with the sh-NC group (Fig. 3A).

In contrast, the proliferation of AGS cells was significantly decreased at 48, 72 and 96 h following transfection with STCAT16 overexpressing vector Fig. 3B).

A colony formation assay produced similar results. Following sh-STCAT16 transfection, BGC-823 cells exhibited a significantly increased number of colonies (Fig. 3C and D).
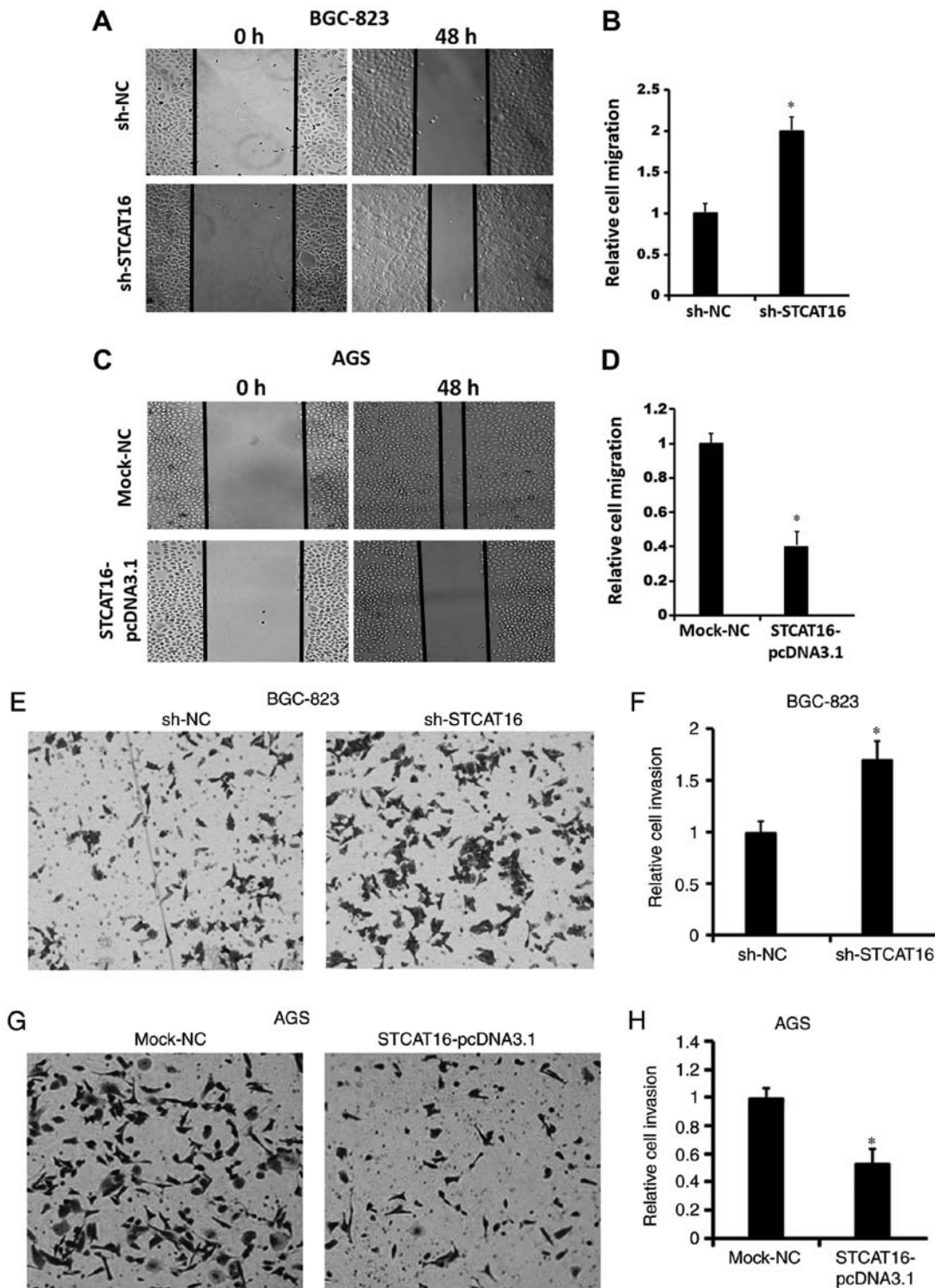
Figure 4. Expression level of STCAT16 affects cell migration and invasion *in vitro*. (A) Wound healing assay in BGC-832 cells following STCAT16 knockdown and (B) corresponding quantification. (C) Wound healing assay in AGS cells following STCAT16 overexpression and (D) corresponding quantification. Magnification, x100. (E) Invasion assay in BGC-832 cells following STCAT16 knockdown and (F) corresponding quantification. (G) Invasion assay in AGS cells following STCAT16 overexpression and (H) corresponding quantification. Representative images of invaded cells are presented. Magnification, x400. Cells in the sh-STCAT16 group were transfected with STCAT16-shRNA-759. *$P<0.05$ vs. corresponding control. STCAT16, stomach cancer-associated transcript 16; sh, short hairpin RNA; NC, negative control.

Conversely, following STCAT16-pcDNA3.1 transfection, AGS cells exhibited a significantly decreased number of colonies compared with the mock-NC group (Fig. 3E and F).

STCAT16 overexpression suppresses gastric cancer cell migration and invasion in vitro. To investigate cell migration

and invasion, wound healing assays and a Matrigel assays were performed, respectively (Fig. 4). The results obtained from the wound-healing assay and the invasion assay suggested that decreasing the expression level of STCAT16 promoted BGC-823 cells migration (Fig. 4A and B) and invasion (Fig. 4E and F). Conversely, the migration (Fig. 4C and D)
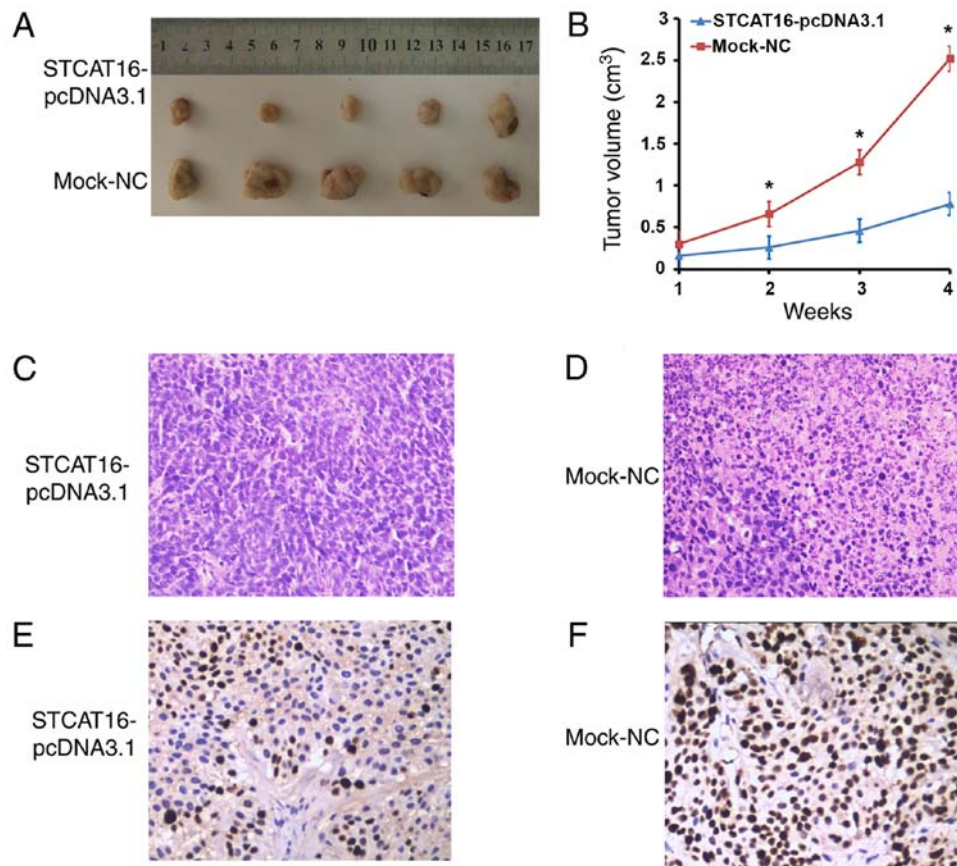
Figure 5. Effects of STCAT16 overexpression on GC cell growth and proliferation *in vivo*. (A) Tumour formation in nude mice at 6 weeks following injection with cells transfected with STCAT16-pcDNA3.1 or mock-NC vectors. (B) Growth curve of tumours derived from cells transfected with STCAT16-pcDNA3.1 or mock-NC vectors. Haematoxylin and eosin staining results in tumours derived from cells transfected with (C) STCAT16-pcDNA3.1 or (D) mock-NC vectors. MKI67 staining results in tumours derived from cells transfected with (E) STCAT16-pcDNA3.1 or (F) mock-NC vectors. Magnification, x400. *P<0.05 vs. corresponding control. GC, gastric cancer; NC, negative control; STCAT16, stomach cancer-associated transcript 16.

and invasion (Fig. 4G and H) of AGS cells were decreased following STCAT16 overexpression.

Overexpression of STCAT16 inhibits tumour progression in BALB/c nude mice. To further investigate the tumour suppressive role of STCAT16, AGS cells transfected with STCAT16-pcDNA3.1 vector or empty vector were injected into BALB/c nude mice. Tumours were detected in all animals injected with AGS cells.

In the mouse xenograft models, the size and the growth of tumours decreased in the STCAT16-pcDNA3.1 group compared with the mock-NC group at 2, 3 and 4 weeks (Fig. 5A and B). Following 4 weeks, the largest tumours exhibited a volume of 3,005.6 and 1,188.1 mm^3 in the STCAT16-pcDNA3.1 group and in the mock-NC group, respectively. The xenografts were fixed with formalin, embedded in paraffin, stained with haematoxylin and eosin (H&E), and incubated with MKI67 antibody. H&E staining indicated that the tumor tissue in the STCAT16-pcDNA3.1 transfected group had a smaller area of necrosis, higher differentiation, less pleomorphism and fission, comparing with that in mock-NC group (Fig. 5C and D). Furthermore, tumours derived from cells transfected with STCAT16-pcDNA3.1 exhibited reduced growth compared with the mock group (4.21±0.90 and 9.80±1.23, respectively, P<0.05; Fig. 5E and F). The

present result suggested that overexpression of STCAT16 significantly inhibited tumour growth in BALB/c nude mice.

Discussion

Accumulating evidence (28,29) has demonstrated that the dysregulation of lncRNAs is involved in the occurrence and development of GC and may promote tumour invasion and metastasis. The overexpression of the lncRNA HOTAIR in GC cells was identified to be associated with TNM stages and lymph node metastasis and to promote colony formation and hepatic metastasis (30). In contrast, knockdown of HOTAIR was identified to reverse epithelial-mesenchymal transition by regulating the expression levels of matrix metalloproteinase (MMP)1 and 3 (31). The upregulation of the lncRNA GHET1 was identified to be associated with gastric tumour growth and invasion and GHET1 overexpression increased the proliferation of GC cells by promoting the interaction between the transcript of MYC proto-oncogene, bHLH transcription factor (MYC) and insulin like growth factor 2 mRNA binding protein 1 (17). HULC expression was identified in hepatocellular cancer; however, it was also demonstrated to be upregulated in GC (32). Additionally, HULC promoted lymph node metastasis and distant metastasis and was identified to be associated with advanced GC (18). A previous study demonstrated that the lncRNA CCAT1 promoted GC progression by upregulating

the expression level of MYC (19). The downregulation of the lncRNA growth arrest specific 5 inhibited the proliferation and induced the apoptosis of GC cells by regulating the activities of cyclin dependent kinase inhibitor 1A and E2F transcription factor 1 (33). The lncRNA GATA6 antisense RNA 1 (head to head) was identified to be downregulated in GC, and its downregulation may lead to tumour-associated phenotypes and metastasis by regulating the expression level of MMP9 (34). The downregulation of the lncRNA MEG3 was demonstrated in GC tissues *in vitro* and *in vivo* (20,35).

In the present study, the expression level of the novel lncRNA STCAT16 was significantly downregulated in GC and was identified to be associated with poor clinical features. STCAT16 was additionally downregulated in GC cell lines. The downregulation of STCAT16 promoted cellular proliferation, migration and invasion, and colony formation *in vitro*. Notably, these effects were reversed following overexpression of STCAT16. *In vivo*, the tumour sizes in the mice injected with cells overexpressing STCAT16 were decreased compared with tumours derived from cells transfected with an empty vector. Furthermore, overexpressing STCAT16 significantly inhibited tumour cell proliferation in BALB/c nude mice. Collectively, the present results suggested that STCAT16 may serve as a tumour suppressor in GC.

Following the identification of dysregulated lncRNAs in GC, it is required to investigate the mechanisms underlying the function of these noncoding RNAs in tumour development and progression. In previous studies, lncRNAs were identified to serve multiple roles by altering gene expression at the transcriptional, by interacting with mRNA molecules, and post-transcriptional levels, by binding to promoter regions (36-38). Additionally, lncRNAs may be involved in post-translational regulation by directly binding to certain proteins involved in tumour progression (36-38). STCAT16 may act as an oncosuppressor via the discussed mechanisms. Further studies are required to investigate the molecular mechanism underlying STCAT16 function in GC.

Acknowledgements

Availability of data and materials

All data generated or analysed during this study are included in this published article.

Authors' contributions

JFZ, WJ, ZBM and ZWW conceived and designed the study. JFZ, WJ, QFZ and XLK performed the experiments. JFZ and WJ wrote the manuscript. ZBM and ZWW reviewed and edited the manuscript. All authors read and approved the manuscript and agree to be accountable for all aspects of the research in ensuring that the accuracy or integrity of any part of the work are appropriately investigated and resolved.

Ethics approval and consent to participate

Ethical approval was obtained from the independent ethics committees at Affiliated Hospital of Nantong University. All patients provided written informed consent.

Patient consent for publication

Not applicable.

Competing interests

The authors declare that they have no competing interests.

References

1. Siegel RL, Miller KD and Jemal A: Cancer statistics, 2018. CA Cancer J Clin 68: 7-30, 2018.
2. Bray F, Ferlay J, Soerjomataram I, Siegel RL, Torre LA and Jemal A: Global cancer statistics 2018: GLOBOCAN estimates of incidence and mortality worldwide for 36 cancers in 185 countries. CA Cancer J Clin 68: 394-424, 2018.
3. Siegel RL, Miller KD and Jemal A: Cancer statistics, 2017. CA Cancer J Clin 67: 7-30, 2017.
4. Chen W, Zheng R, Baade PD, Zhang S, Zeng H, Bray F, Jemal A, Yu XQ and He J: Cancer statistics in China, 2015. CA Cancer J Clin 66: 115-132, 2016.
5. Nie Y, Wu K, Yu J, Liang Q, Cai X, Shang Y, Zhou J, Pan K, Sun L, Fang J, *et al*: A global burden of gastric cancer: The major impact of China. Expert Rev Gastroenterol Hepatol 11: 651-661, 2017.
6. Li Q, Chen C, Kapadia A, Zhou Q, Harper MK, Schaack J and LaBarbera DV: 3D models of epithelial-mesenchymal transition in breast cancer metastasis: High-throughput screening assay development, validation, and pilot screen. J Biomol Screen 16: 141-154, 2011.
7. Gupta GP and Massagué J: Cancer metastasis: Building a framework. Cell 127: 679-695, 2006.
8. Klein CA: Cancer. The metastasis cascade. Science 321: 1785-1787, 2008.
9. Mercer TR and Mattick JS: Structure and function of long noncoding RNAs in epigenetic regulation. Nat Struct Mol Biol 20: 300-307, 2013.
10. Wang C, Wang L, Ding Y, Lu X, Zhang G, Yang J, Zheng H, Wang H, Jiang Y and Xu L: LncRNA structural characteristics in epigenetic regulation. Int J Mol Sci 18: pii: E2659, 2017.
11. Vance KW and Ponting CP: Transcriptional regulatory functions of nuclear long noncoding RNAs. Trends Genet 30: 348-355, 2014.
12. Yoon JH, Abdelmohsen K and Gorospe M: Posttranscriptional gene regulation by long noncoding RNA. J Mol Biol 425: 3723-3730, 2013.
13. Huang JZ, Chen M, Chen, Gao XC, Zhu S, Huang H, Hu M, Zhu H and Yan GR: A peptide encoded by a putative lncRNA HOXB-AS3 suppresses colon cancer growth. Mol Cell 68: 171-184.e6, 2017.
14. Huarte M and Rinn JL: Large non-coding RNAs: Missing links in cancer. Hum Mol Genet 19: R152-R161, 2010.
15. Pan W, Liu L, Wei J, Ge Y, Zhang J, Chen H, Zhou L, Yuan Q, Zhou C and Yang M: A functional lncRNA HOTAIR genetic variant contributes to gastric cancer susceptibility. Mol Carcinog 55: 90-96, 2016.
16. Liu XH, Sun M, Nie FQ, Ge YB, Zhang EB, Yin DD, Kong R, Xia R, Lu KH, Li JH, *et al*: Lnc RNA HOTAIR functions as a competing endogenous RNA to regulate HER2 expression by sponging miR-331-3p in gastric cancer. Mol Cancer 13: 92, 2014.

17. Yang F, Xue X, Zheng L, Bi J, Zhou Y, Zhi K, Gu Y and Fang G: Long non-coding RNA GHET1 promotes gastric carcinoma cell proliferation by increasing c-Myc mRNA stability. FEBS J 281: 802-813, 2014.
18. Zhao Y, Guo Q, Chen J, Hu J, Wang S and Sun Y: Role of long non-coding RNA HULC in cell proliferation, apoptosis and tumor metastasis of gastric cancer: A clinical and *in vitro* investigation. Oncol Rep 31: 358-364, 2014.
19. Yang F, Xue X, Bi J, Zheng L, Zhi K, Gu Y and Fang G: Long noncoding RNA CCAT1, which could be activated by c-Myc, promotes the progression of gastric carcinoma. J Cancer Res Clin Oncol 139: 437-445, 2013.
20. Peng W, Si S, Zhang Q, Li C, Zhao F, Wang F, Yu J and Ma R: Long non-coding RNA MEG3 functions as a competing endogenous RNA to regulate gastric cancer progression. J Exp Clin Cancer Res 34: 79, 2015.
21. Xu G, Meng L, Yuan D, Li K, Zhang Y, Dang C and Zhu K: MEG3/miR-21 axis affects cell mobility by suppressing epithelial-mesenchymal transition in gastric cancer. Oncol Rep 40: 39-48, 2018.
22. Iyer MK, Niknafs YS, Malik R, Singhal U, Sahu A, Hosono Y, Barrette TR, Prensner JR, Evans JR, Zhao S, *et al*: The landscape of long noncoding RNAs in the human transcriptome. Nat Genet 47: 199-208, 2015.
23. In H, Solsky I, Palis B, Langdon-Embry M, Ajani J and Sano T: Validation of the 8th edition of the AJCC TNM staging system for gastric cancer using the national cancer database. Ann Surg Oncol 24: 3683-3691, 2017.
24. Livak KJ and Schmittgen TD: Analysis of relative gene expression data using real-time quantitative PCR and the 2(-Delta Delta C(T)) method. Methods 25: 402-408, 2001.
25. Zhang JF, Qu LS, Qian XF, Xia BL, Mao ZB and Chen WC: Nuclear transcription factor CDX2 inhibits gastric cancer-cell growth and reverses epithelial-to-mesenchymal transition *in vitro* and *in vivo*. Mol Med Rep 12: 5231-5238, 2015.
26. Guo P, Wang J, Gao W, Liu X, Wu S, Wan B, Xu L and Li Y: Salvianolic acid B reverses multidrug resistance in nude mice bearing human colon cancer stem cells. Mol Med Rep 18: 1323-1334, 2018.
27. Zhang J, Ding W, Kuai X, Ji Y, Zhu Z, Mao Z and Wang Z: Dermcidin as a novel binding protein of lncRNA STCAT3 and its effect on prognosis in gastric cancer. Oncol Rep 40: 2854-2863, 2018.
28. Abbastabar M, Sarfi M, Golestani A and Khalili E: lncRNA involvement in hepatocellular carcinoma metastasis and prognosis. EXCLI J 17: 900-913, 2018.
29. Gong P, Qiao F, Wu H, Cui H, Li Y, Zheng Y, Zhou M and Fan H: LncRNA UCA1 promotes tumor metastasis by inducing miR-203/ZEB2 axis in gastric cancer. Cell Death Dis 9: 1158, 2018.
30. Shao Y, Chen H, Jiang X, Chen S, Li P, Ye M, Li Q, Sun W and Guo J: Low expression of lncRNA-HMlincRNA717 in human gastric cancer and its clinical significances. Tumour Biol 35: 9591-9595, 2014.
31. Xu ZY, Yu QM, Du YA, Yang LT, Dong RZ, Huang L, Yu PF and Cheng XD: Knockdown of long non-coding RNA HOTAIR suppresses tumor invasion and reverses epithelial-mesenchymal transition in gastric cancer. Int J Biol Sci 9: 587-597, 2013.
32. Klec C, Gutschner T, Panzitt K and Pichler M: Involvement of long non-coding RNA HULC (highly up-regulated in liver cancer) in pathogenesis and implications for therapeutic intervention. Expert Opin Ther Targets 23: 177-186, 2019.
33. Liu L, Yan B, Yang Z, Zhang X, Gu Q and Yue X: ncRuPAR inhibits gastric cancer progression by down-regulating protease-activated receptor-1. Tumour Biol 35: 7821-7829, 2014.
34. Park SM, Park SJ, Kim HJ, Kwon OH, Kang TW, Sohn HA, Kim SK, Moo Noh S, Song KS, Jang SJ, *et al*: A known expressed sequence tag, BM742401, is a potent lincRNA inhibiting cancer metastasis. Exp Mol Med 45: e31, 2013.
35. Dan J, Wang J, Wang Y, Zhu M, Yang X, Peng Z, Jiang H and Chen L: LncRNA-MEG3 inhibits proliferation and metastasis by regulating miRNA-21 in gastric cancer. Biomed Pharmacother 99: 931-938, 2018.
36. Moran VA, Perera RJ and Khalil AM: Emerging functional and mechanistic paradigms of mammalian long non-coding RNAs. Nucleic Acids Res 40: 6391-6400, 2012.
37. Wu J and Hann SS: Functions and Roles of long-non-coding RNAs in human nasopharyngeal carcinoma. Cell Physiol Biochem 45: 1191-1204, 2018.
38. Batista PJ and Chang HY: Long noncoding RNAs: Cellular address codes in development and disease. Cell 152: 1298-1307, 2013.